DOI: 10.24850/j-tyca-2022-03-04

Articles

Geometry determination of the hydrogeologic basement in the Interserrana Basin through VES

Determinación de la geometría del basamento hidrogeológico en la Cuenca Interserrana mediante SEV

Gaston Mendoza-Veirana[1], ORCID: https://orcid.org/0000-0002-1030-8485

Santiago Perdomo[2], ORCID: https://orcid.org/0000-0003-0957-6068

Jerónimo Ainchil[3], ORCID: https://orcid.org/0000-0001-9075-4698

[1]Ghent University, Faculty of Bioscience Engineering, Department of Environment. Coupure Links 653, geb. B, 9000, Ghent, Belgium/ The National University of La Plata, School of Astronomical and Geophysical Sciences. Paseo del Bosque s/n, La Plata (B1900), Buenos Aires, Argentina, gaston.mendozaveirana@ugent.be

[2]National University of Northwestern Buenos Aires, Research and Transference Centre of Northwestern Buenos Aires, National Scientific and Technical Research Council. Monteagudo 2772, Pergamino (B2700), Buenos Aires, Argentina. sperdomo@comunidad.unnoba.edu.ar

[3]The National University of La Plata, School of Astronomical and Geophysical Sciences. Paseo del Bosque s/n, La Plata (B1900), Buenos Aires, Argentina. jero@fcaglp.unlp.edu.ar

Corresponding author: Gaston Matias Mendoza-Veirana, mendoveirana@gmail.com

Abstract

This paper shows a geoelectric exploration of the southwest sector of the Interserrana Basin, Province of Buenos Aires, Argentina. Due to the relative scarcity of regional studies carried out in the zone, a more detailed understanding of its geological structures and aquifers makes an important contribution to addressing environmental and productivity challenges. The objective is to obtain a depth section of the resistive hydrogeological basement. To meet our objective, we developed a model consisting of the 1D inversion of 49 Schlumberger VES, distributed uniformly along a 139 km route. The inversion process was performed with specific software which implements Zohdy's algorithm (Zohdy, 1989) for the solution of direct and inverse problems. The transition from the 49 one-dimensional inverted profiles to a continuous section was carried out using a machine learning interpolation technique. An uncertainty analysis is also presented, which revealed a correspondence between this feature and the depth obtained for the resistive basement. This trend allowed us to establish a reliability criterion at each true basement-depth value. Finally, we offer a geological interpretation of our results and their correspondence with previous geological research.

Keywords: Hydrogeology, resistivity, aquifer, uncertainty, Interserrana, random forest.

Resumen

El presente trabajo muestra una exploración geoeléctrica del sector suroeste de la Cuenca Interserrana en la provincia de Buenos Aires, Argentina. Debido a la relativa escasez de estudios regionales llevados aquí, un entendimiento más detallado de sus estructuras geológicas y acuíferos conforma un importante aporte al abordar desafíos ambientales y productivos que tienen lugar en la zona. El objetivo propuesto es obtener una sección de la profundidad del basamento hidrogeológico resistivo. Para cumplir con el objetivo desarrollamos un modelo consistente en la inversión 1D de 49 SEV Schlumberger distribuidos uniformemente a lo largo de una ruta de 139 km. El proceso de inversión fue con un *software* específico que implementa el algoritmo de Zohdy (1989) para la solución del problema directo e inverso. El paso de los 49 perfiles unidimensionales de resistividad verdadera a la sección continua se llevó a cabo usando una técnica de interpolación de *machine learning*. También se muestra un análisis de incertidumbre que reveló una correlación lineal entre esta misma característica y la profundidad obtenida para el basamento resistivo. Esta tendencia nos permitió establecer un criterio de confianza en cada valor de profundidad verdadera de basamento. Finalmente ofrecemos una interpretación geológica de los resultados y su correspondencia con los trabajos antecedentes.

Palabras clave: hidrogeología, resistividad, acuífero, incertidumbre, interserrana, bosques aleatorios.

Received: 10/30/2020

Accepted: 28/04/2021

Introduction and objectives

The underground flow in shallow aquifers is part of the hydrological cycle, and its variability is affected by recharging processes and human intervention (Poland, 1984). Groundwater levels in many of the world's aquifers have been trending downwards in recent years, generally due to that groundwater pumping is carried out at a faster rate than its recharging (Barends, Brouwer, & Schröder, 1995).

The Interserrana Basin (IB) is a geological basin between the Sierras de Tandilia to the northeast (NE) and Ventania to the southwest (SW), Province of Buenos Aires, Argentina. The soil and climate conditions in this area generate an optimal environment for agricultural production so this is one of the most productive zones in the country. This activity is highly dependent on the availability of both surface and underground water resources (Llambías & Prozi, 1975; Kruse, 1993; Kruse, Varela, Laurencena, & Deluchi, 1998; Campo-de-Ferreras & Piccolo, 2002; Quiroz-Londoño, Martínez, & Massone, 2012). Although there are geoelectric exploration studies in this area (Weinzettel, Varni, & Usunoff, 2005; Quiroz-Londoño, Martínez, Massone, Bocanegra, & Ferrante,2006; Varni, Weinzettel, & Usunoff, 2010; Giaconi, Amboni, & Giaconi, 2014; Sierra, Weinzettel, Dietrich, Bea, & Cacciabue, 2016), they are rather only local ones, so that regional studies are scarce (Weinzettel & Varni, 2007) and mainly focused on the Claromeco Basin, which is part of the IB. Deep drillings that reach the basement are insufficient to adequately characterize the availability of underground water reserves. In this sense, geophysical studies are a fundamental tool for regional studies.

To explore the depth variations of the impermeable hydrological basement that limits the aquifer systems, 49 vertical electrical soundings (VES) were carried out in Schlumberger mode. The application of this technique is of vital interest due to the resistivity contrast that could exist between the resistive-impermeable basement and sedimentary formations. In addition to providing verifiable and replicable evidence of known reliability, VES is a relatively inexpensive method compared to the process of drilling exploratory wells. The soundings were carried out throughout a route of 139 km and inverted with SEV's software (Nigro & Perdomo, 2017) to infer the depth of the basement with a tolerance of the root mean square error (RMSE) less than or equal to 5%. This has allowed us to obtain a geoelectric section, interpolated through the machine learning algorithm called random forests (Breiman, 2001).

Study area and hydrogeology

The study area (Figure 1) corresponds to a profile of 139 km long in the Province of Buenos Aires (Argentina) on which 49 VES were carried out, with distances between two and four kilometers between each one (37 ° 59 '- 38 ° 38' South and 60 ° 04 '- 60 ° 55' West). This profile is found in the southwestern portion of the IB, comprising the towns of Gonzales Cháves to the north, Tres Arroyos to the center, and the surroundings of Jose Guiasola to the SW.

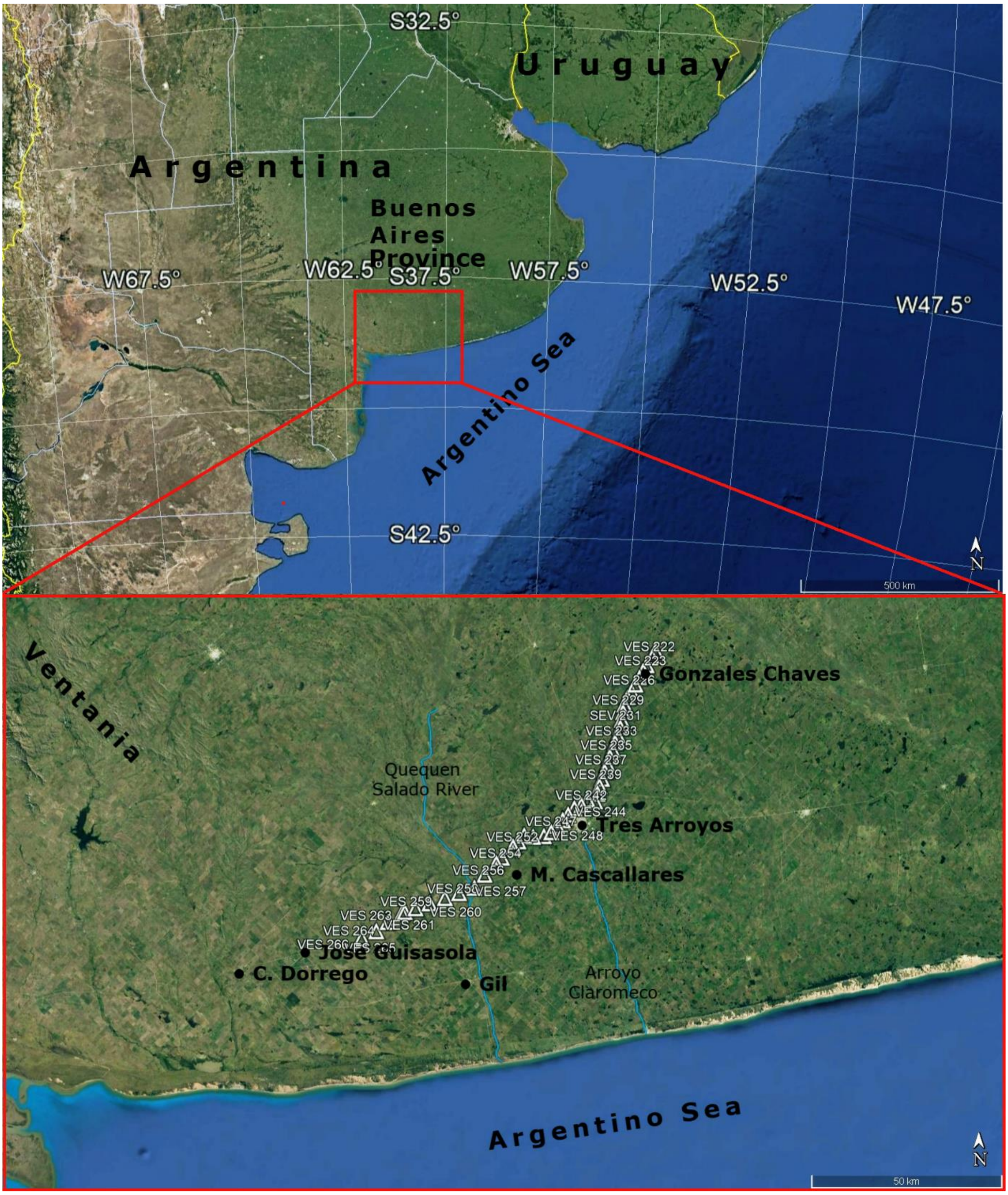

Figure 1. Each white icon represents the coordinates of a VES. Major cities and geographic references are included.

From the hydrogeological point of view, we can distinguish four large sections: Paleozoic impermeable basement, Hipoparaniana Section (Olivos Formation), Paraniana Section (Paraná Formation) and Epiparaniana Section (Sala, 1975; Hernández, Filí, Auge, & Ceci, 1979). Regarding the exploitation of the aquifers, the Epiparaniana constitutes a multi-unit aquifer, which upper productive horizon is phreatic. The water table is the main source of exploitation, both for agricultural use and for supply in small towns. In the most important populated areas, drilling has been made at deeper productive levels, some of them semi-confined ((Sala & Cavalié, 1993). The latter is done also to reduce the most common risk of contamination that emerges in the surface layers, due to anthropic activity (Weinzettel *et al*., 2005).

According to García (1969), González (2005), Harrington (1970), Terraza y Deguillén (1973), Weinzettel and Varni (2007) the basement outcrops in sectors close to the town of Gonzales Cháves, is identified as a Paleozoic rock of quartz-clayey schist. As we approach the marine coast, the depth of the basement increases reaching values on the scale of hundreds of meters.

The Hipoparaniana Section is very limited in its thickness. It is composed of intercalations of fine clayey sandstones and reddish-brown clays, it is arranged on angular unconformity on the quartzites, being its erosion layer on which the Paraniana Section sits. From the hydrogeological point of view, this section is considered aquitard with aquifer intercalations, but with high-salinity-levels water (Hernández *et al*., 1979; Sala & Cavalié, 1993).

The Paraniana Section includes marine deposits and is vertically limited by surfaces of erosional unconformity. They are clays, clayey sandstones, and fine-grain sand somewhat gypsumish, green-greyish, and bluish, with marine fossils (Sala, 1975). In the city of Gil, there are 45 m of fine-grain sand over 247 m of compact clays, linking the section directly with the Epiparaniana (Sala & Cavalié, 1993).

The Epiparaniana Section is made up of Araucanian deposits (clayey and finely calcareous sandstones), Pampean (loessoid sandy silts), post-Pampean, dunes, alluviums and soils; the first two of which are of hydrological interest (Hernández *et al*., 1979).

Regarding exploratory drilling, just one has been identified on the surroundings of the study area, more precisely in the city of Gil (Dirección Nacional de Geología y Minería, 1970). On the basis of which a stratigraphic column has been built (Figure 2), where the four hydrogeological sections mentioned above are identified. The same well's register shows a chemical analysis among which the salinity of the different sedimentary formations stands out. This analysis shows the highest concentration of sodium chloride in the section interpreted as Hipoparaniana. Finally, regarding the target basement, there exist just one regional geoelectric study known to date (see Figure 4 in Weinzettel & Varni, 2007). It shows the location of the schist-quartz basement at 426 m below the wellhead in the city of Gil. As well as in Ramos (1999), a description of the regional geology shows tertiary sediments deposited on Neopaleozoic deposits, with a deepening trend toward the SW in their structural context.

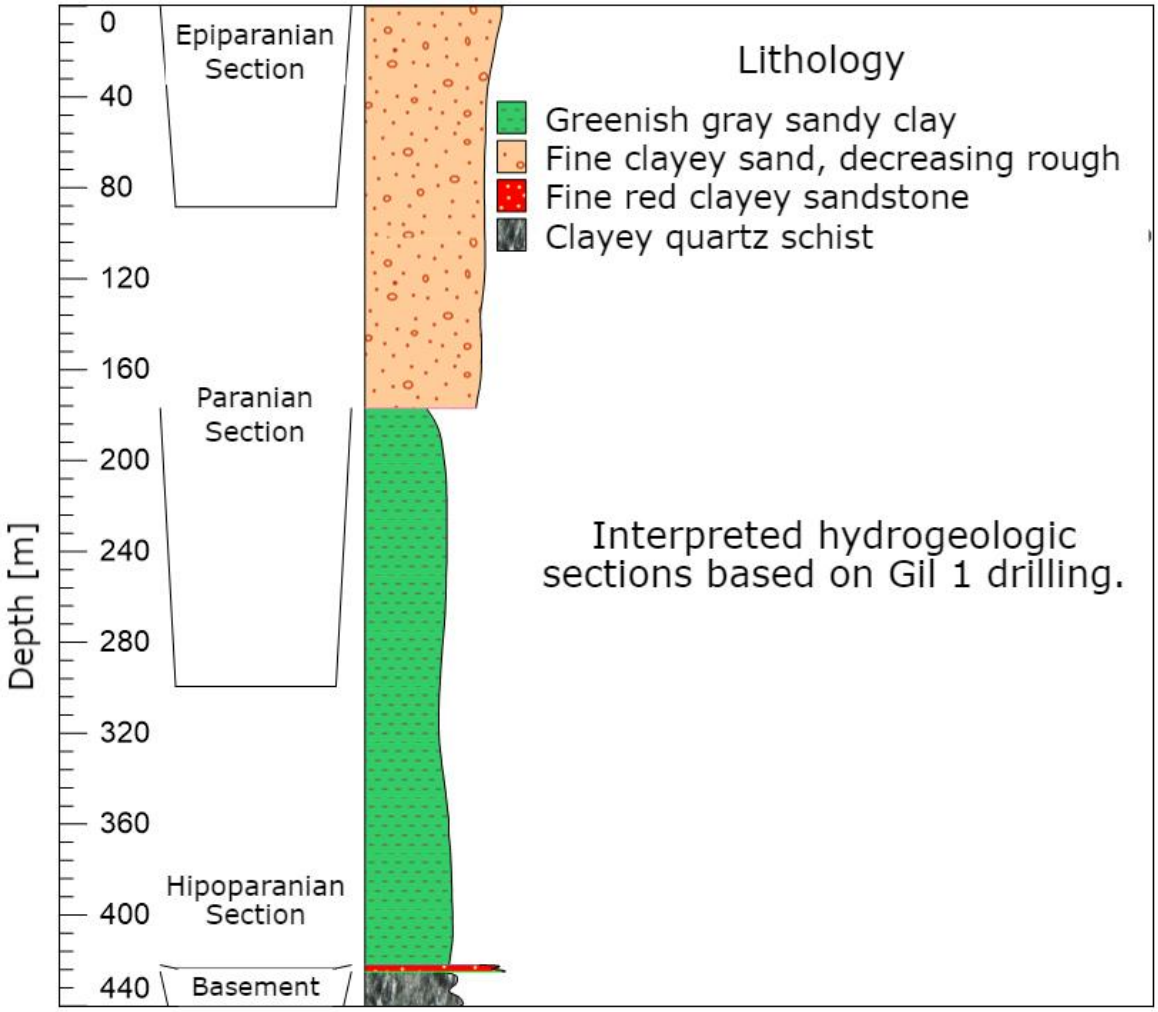

Figure 2. Interpretation of hydrogeological sections based on well drilling Gil 1 (Dirección Nacional de Geología y Minería, 1970). The basement is only reached less than a meter deep in the bottom hole, here it is shown extended.

Methodology

As usual, when modeling the subsoil using VES, it is assumed that the layers below the central point of the array are flat and discrete, homogeneous and isotropic, parallel and infinite laterally of constant resistivity. The measured soundings were carried out in the Schlumberger tetra electrode mode. For each VES, the maximum distance AB/2 varies between 100 and 500 m. This was based on the apparent resistivity values observed in the field, also called the observed apparent resistivity curve (OARC). We worked with the assumption that when at least 3 apparent resistivity values reach the asymptote of 45 degrees of inclination, it is considered that the observed contrast is sufficient to infer the presence of the resistive (target) basement, and therefore the AB/2 distance is sufficient to interpret it (Orellana, 1982). The data processing was carried out using the SEV's software (Nigro & Perdomo, 2017) which implements Zohdy's algorithm (Zohdy, 1989) for the resolution of the inverse problem. The latter uses the convolution method and digital filtering theory (Johansen, 1975), based on the solution of Stefanesco, Schlumberger and Schlumberger (1930); while the resistivity transform is calculated using Sunde's algorithm (Sunde, 1949). The number of true layers was manually reduced by Dar Zarrouk's method (Maillet, 1947). So that the difference between the OARC and the calculated apparent resistivity curve (CARC) has a tolerance of RMSE = 5 %. A value of 100 Ohm.m was set for the hydrogeological basement, due to the geological antecedents, well observations, and the measured contrasts of resistivities. This value is a higher order of magnitude than the observed apparent resistivity of the sediments above the basement; this hypothesis allows us to explain the asymptotic growth at 45 degrees for an OARC when a resistive basement is reached (Orellana, 1982).

Despite the existence of VES inversion methods using artificial neural networks which have demonstrated their superior adjustment capacity compared to Zohdy's algorithm (Zohdy, 1989) for automatic solutions (Maiti, Gupta, Erram, & Tiwari, 2011; Raj, Srinivas, Oliver, & Muthuraj, 2014), the latter has been chosen in this case. This is because it allows manual adjustment of the layers using Dar Zarrouk's method (Maillet, 1947); being that the objective of this analysis is to focus on the exploration and geological interpretation of the results. Additionally, the non-uniqueness of the solution to the inverse problem added to the fact that the differences in the true resistivity curve (TRC) adjusted by Zohdy's algorithm (Zohdy, 1989) or the artificial neural networks are minimal compared to the restrictions that our models pose, as geological hypotheses have been introduced.

Interpolation

Obtaining a TRC for each VES, the resistivity distribution under the center of the array is represented in a one-dimensional way. This distribution in the form of a profile motivates to interpolate the depths obtained. So that our model becomes a sequence of 49 discrete one-dimensional observations to a continuous section. Based on Prasad, Iverson and Liaw (2006); Li, Heap, Potter and Daniell (2011); Thessen (2016), and Nussbaum *et al*. (2018), the most suitable algorithm to perform this task is the random forests (RF), belonging to the family of machine learning assembly methods. Random forests in regression mode consist of averaging the solutions of a series of decision trees (Breiman, 2001; Louppe, 2014). Standard procedures for training, testing, and choosing parameters that minimize prediction errors were taken from Hastie, Tibshirani and Friedman (2009); Domingos (2012); Mehta *et al*. (2019). The implemented code was written in Python, implementing RF with the Scikit Learn library (Pedregosa *et al*., 2011) and its modules for the implementation of assemblies (https://scikit-learn.org/stable/modules/generated/sklearn.ensemble.RandomForestRegressor.html).

Uncertainty

Since the solutions to the inverse problem are not unique within the proposed tolerance, there are several TRC that can be proposed as the solution to each VES. The depth at which the basement is modeled with the lowest RMSE is called the optimum basement depth (OBD). Then, given a particular VES and its OBD, it is possible to increase or reduce the estimated depth of the basement until obtaining RMSE=5 %. If we take the greater of these two distances and calculate its percentage concerning the OBD, we obtain the maximum percentage uncertainty (MPU). The MPU is then a measure of how much it is possible to vary the true depth of the basement in relation to the OBD, within the accepted tolerance. A low MPU indicates that the OBD is more reliable, while the opposite case indicates greater uncertainty.

Results

Following the methodology and hypotheses set forth in the previous section, we were able to solve 46 of the 49 VES within the proposed tolerance (RMSE ≤ 5 %). The VES 263 and 264 have a good adjustment at considerable depths, but in the first 50 meters, they present significant variations in resistivity, presumably due to the presence of tuff, which did not allow an adjustment within tolerance. But since the target is deeper (500 and 430 meters respectively, taken from the surface) these soundings are included in the results. Finally, the field curve of VES 229 presented some variations in the first sections of the curve that resulted in an adjustment slightly higher than the pre-set tolerance. Figure 3 shows two characteristic curves of the explored area together with their hydrogeological interpretation. As previously argued, based on the homogeneity of the geological area, the resistivity of 100 Ohm.m has been assumed for the resistive basement in all cases. This leads us to model the basement in a rather superficial way while the OARC tends to 45 degrees, as is the case in Figure 3A. And to model deeper basements in areas where the OARC grows slightly even when they are close to the maximum AB/2 (Figure 3B).

A)

AB/2	RA calc	RA obs
2	25,73	25,918
3	27,596	29,452
4	28,037	28,917
5	27,562	26,989
6	26,585	25,918
8	24,141	23,562
10	21,857	21,42
13	19,309	19,492
16	17,667	17,993
20	16,319	16,815
25	15,276	15,315
32	14,253	14,2
40	13,318	13,5
50	12,395	12,2
65	11,588	11,6
80	11,464	11,8
100	12,108	12,4
125	13,669	13,4
160	16,398	16
200	19,629	20,1
250	23,483	24,9

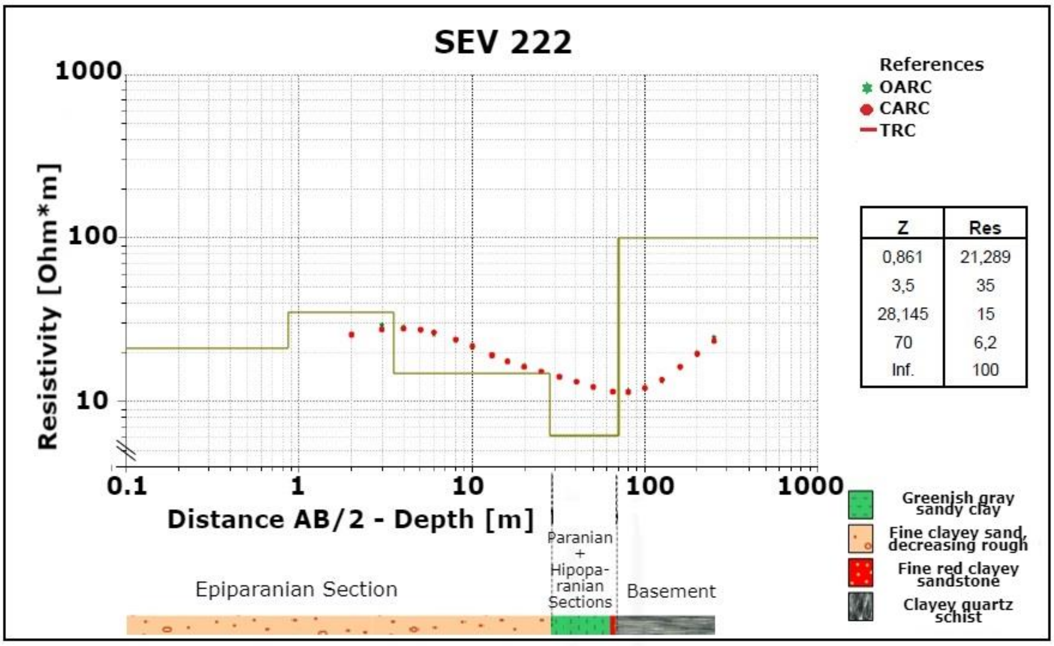

RMSE = 2.673 Lat = -37° 58,575' Long = -60° 3,60822' Top = 202 [m]

B)

AB/2	RA calc	RA obs
2	550,681	501,952
3	507,349	550,56
4	422,375	458,304
5	330,812	350,176
6,5	216,014	221,216
8	137,976	134,912
10	78,661	70,432
13	41,401	39,581
16	28,43	28,966
20	21,815	22,518
25	17,942	18,352
32	14,847	14,7
40	12,665	12,4
50	10,867	10,8
65	9,101	8,9
80	7,947	7,7
100	6,955	6,9
125	6,218	6,3
160	5,676	5,5
200	5,396	5,3
250	5,279	5,2
320	5,321	5,2
400	5,534	5,5
500	5,966	5,9

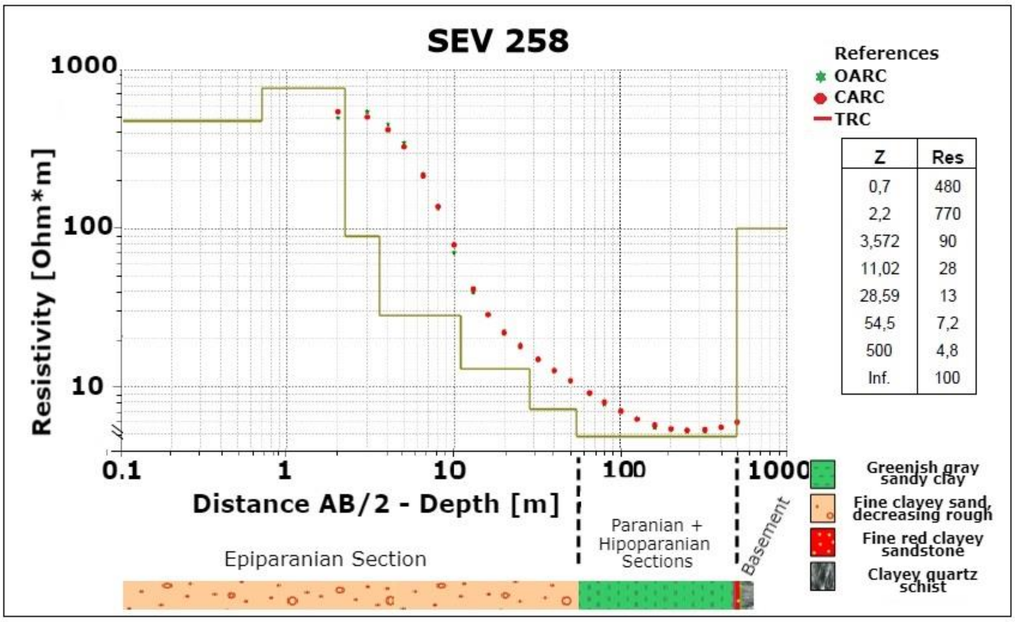

RMSE = 4.476 Lat = -38° 32,24718' Long = -60°3,60822' Top = 91 [m]

Figure 3. OARC, CARC, TRC, and hydrogeological interpretation for the VES 222 (A) and 258 (B) characteristics of the section in the NE and SW sectors respectively. Note that the horizontal scale is logarithmic also for

hydrogeological sections.

The overall average fit is RMSE = 3.78 % for all the VES. The results of the inversion can be seen in Figure 4. In the northeast sector, the basement is closer to the surface, beginning at 170 meters above sea level and continuing with an irregular deepening that reaches -480 meters above sea level in the southwest sector.

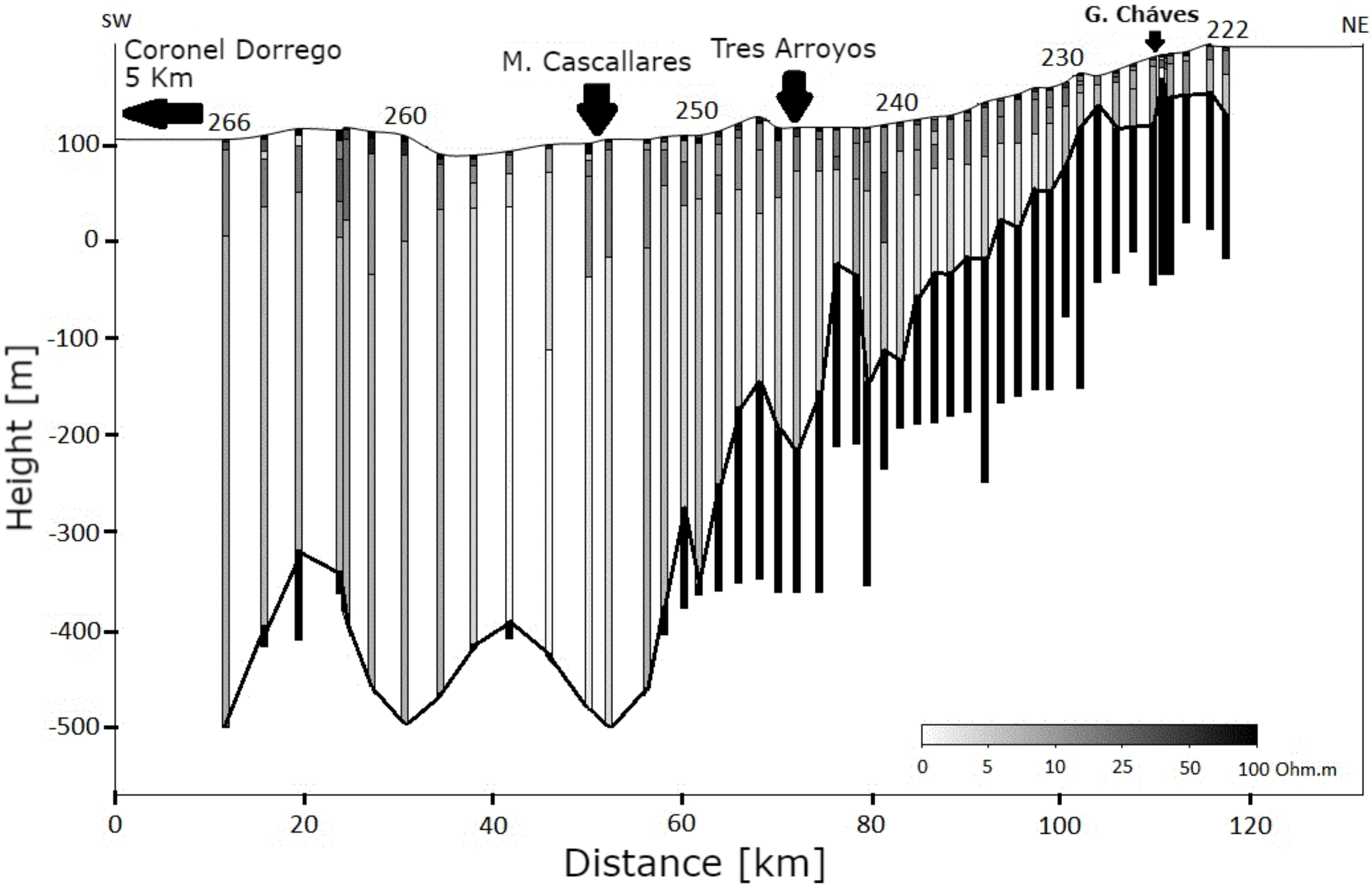

Figure 4. Results of the 49 inverted VES with their regional references, resistivity, and depth. The black curve represents the modeled depth for the resistive basement.

Continuous section

The adjustment of the RF algorithm has been very good; the training and testing errors are around 96 % (variance reduction). The chosen parameters are those that minimize the expected testing error, averaged over one hundred random 80-20 partitions of the original data. Next, we detail the optimal parameters that we have found and used in the application of the algorithm. Latitude and longitude as training variables, depth of trees without pruning, two minimum samples, and only one characteristic considered per node. As is usual by default in Scikit Learn (Pedregosa *et al*., 2011), 500 trees have been used in the forest. Figure 5 shows in orange the basement depth interpolations obtained by VES.

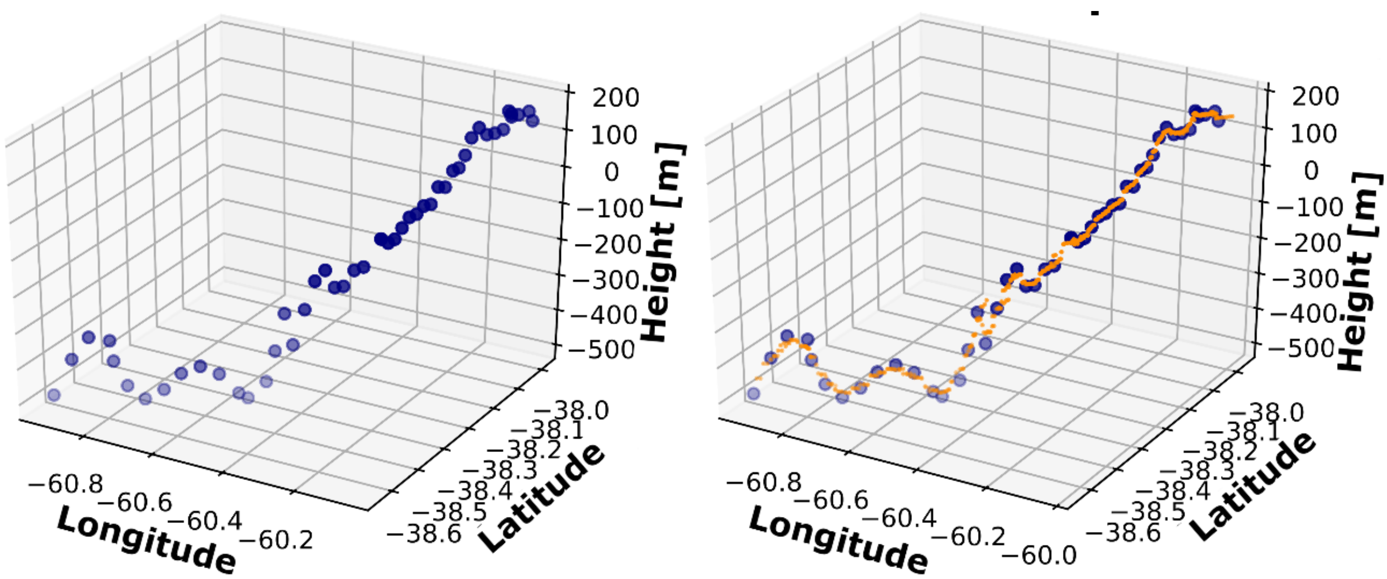

Figure 5. Three-dimensional representation of the true basement depths obtained by VES. The image on the left shows in blue the heights taken from the reference ellipsoid. The image on the right adds in orange the

interpolated values obtained through the optimal implementation of random forest.

Uncertainty analysis

As described in the uncertainty section, the MPU of each VES was calculated. As an example, Figure 6 shows part of the SEV's software interface for VES 248. The depth differences are calculated concerning its OBD (270 m). If we propose the basement at 250 or 320 m, we reach the proposed tolerance. As 320 m is the longest difference concerning the OBD (270 m), we obtain an MPU of 18 % (270 m ± 50 m).

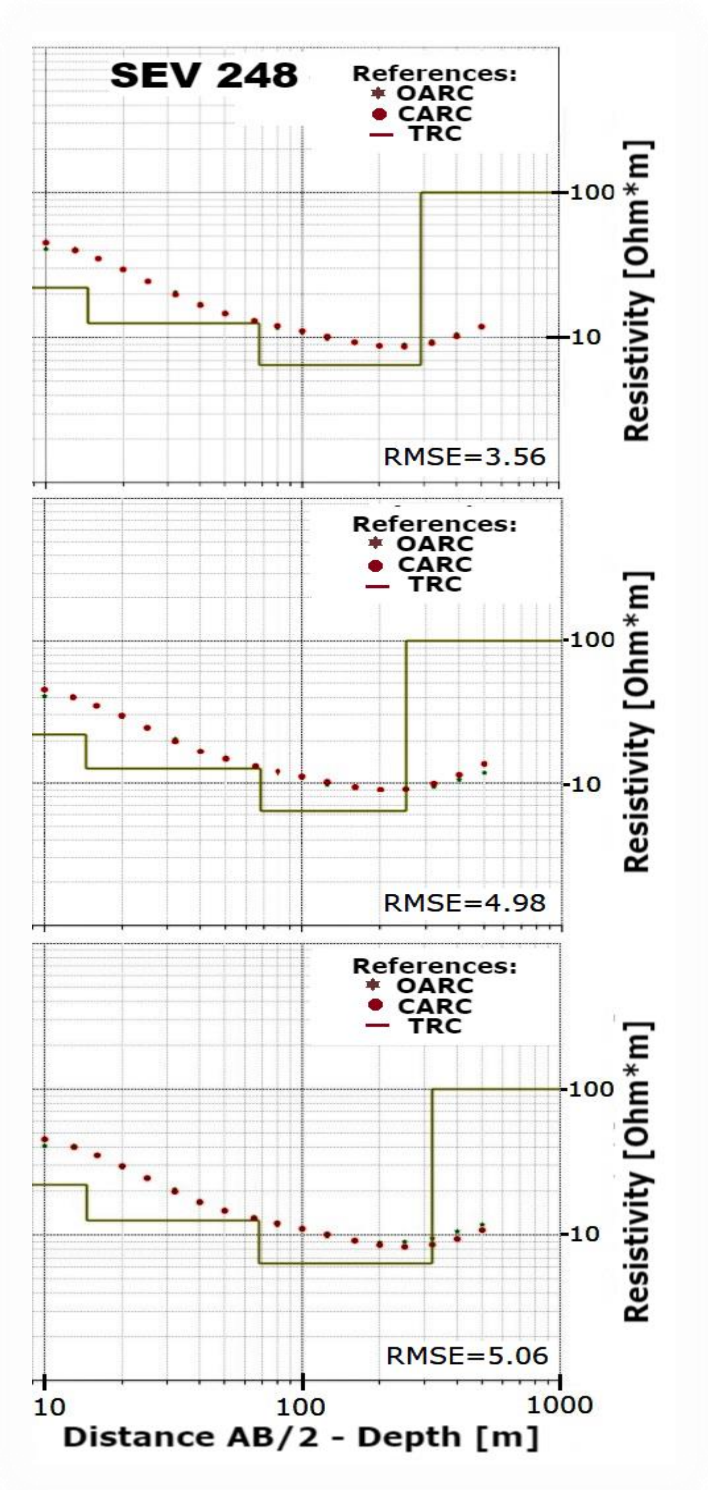

Figure 6. The VES 248 has its OBD at 270 meters, with an RMSE = 3.6 % (upper figure). By reducing the true depth of the basement, to 250 meters we reach the proposed tolerance (center figure), similarly at 320 meters if

we increase the depth (lower figure).

Once the MPU for each VES was obtained, as can be seen in Figure 7, we graph them for the OBD. There is a clear linear trend between both properties. The dispersion of the values also grows with the OBD. A linear regression line using least squares was fitted to model the trend, which seems to disappear for OBD greater than 400 m.

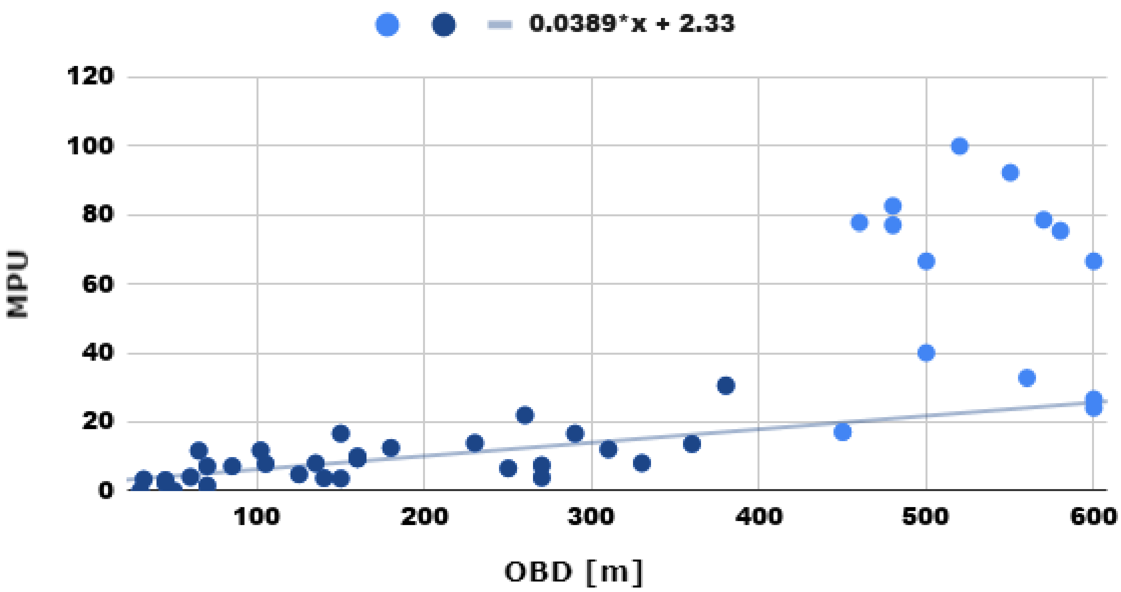

Figure 7. The graph shows the MPU about the OBD for each of the VES. A linear function is calculated for values less than 400 m of OBD (in dark blue) and extrapolated to the rest of the graph (in light blue).

Discussion and interpretation

Figure 4 shows that above the basement a layer of low resistivity, which varies between 2.6 and 13.3 Ohm.m and 10 to 500 m of thickness, can be distinguished. This layer is the one interpreted as Paranian and Hipoparanian Section in Figure 3. Since the Hipoparaniana Section is of reduced thickness to the other hydrogeological sections, it has not been possible to be distinguished. As presented in the section on hydrogeology, the Paraniana has large thicknesses added to low resistivities because of its salinity. This section visible in Figure 4 has been associated with the combination of both tertiary sections. Additionally, considering the antecedent geoelectric work on a regional scale by Winzettel and Varni (2007) (see Figure 4 of the aforementioned work) we can effectively correlate both results. This is for both the depth of the basement and the thickness of the Paraniana Section. This same regional trend of the Paleozoic rock deepening towards the SW, which subscribes to tertiary sediments, is also qualitatively described by Ramos (1999) in its structural context.

Based on the OBD found, the interpolation technique used is the one with the best adjustment known, since the model can predict values for which it was not trained with an expected score of 96 %. This allows us to obtain a continuous distribution of our objective. However, the fact of having interpolated in longitude and latitude, not in planar coordinates, should be noted as a limitation; since when the interpolation is performed latterly, we cannot ensure a priori that random forest is the most suitable method.

As seen in the previous section, there is a clear correlation between the MPU and the OBD, with a Pearson coefficient of 0.8. The VES with an MPU greater than 40 % is clearly outside the proposed trend. This can be explained by considering the few deep observations that VES 254, 255, 256, 259, 260, 261, 262, 265, and 266 possess. That is, in the observations made using distances AB/2 of 500 m, despite being able to notice the presence of the basement, they are insufficient to model it within the expected uncertainty. Longer distances AB/2 are necessary to model the basement with less uncertainty.

Conclusions

The objective proposed in the first section has been widely met. The present study was performed on a regional scale and presents a density of observations at least double that of the previous works. This constitutes an important contribution to the knowledge of the aquifer's structure in the Interserrana Basin.

The geological hypotheses introduced based on the antecedent studies, allowed us to effectively find the OBD of all the VES, within the proposed tolerance, except for one case. Additionally, these discrete observations were interpolated under the best current standards.

The hydrogeological basement has shallow depths towards the NE, in correspondence with the Gonzales Chávez outcrop. Continuing with a progressive deepening towards the SW reaching maximum values of 600 m crossing the Quequén Salado River. It was also possible to identify and correlate the Hipoparaniana and Paraniana Sections in the results shown in Figure 4. Resistivity values greater than 10 Ohm.m above the basement could be indicating the presence of freshwater aquifers, as shown by the Chemical analysis of the Gil-1 well for salinity. Which in particular shows an increase with the depth of the sediments, a fact reflected in the TRC of Figure

4.

As limitations of the present study, we can mention what was discussed in the previous section about interpolation using longitude and latitude. As well as there are no deep drillings next to the VES, to be considered as a reference for adjusting the geoelectric models. Despite this, the models presented here satisfy all the geological and hydrogeological evidence published about the area and comply with the processing standards.

The results of the uncertainty analysis together with the trend found for the basement, have allowed us to propose recommendations for field tasks to minimize the uncertainty of the OBD. Thus, obtaining an even more reliable basement model. Finally, due to the great utility of this analysis, it is desirable that the linear trend be confirmed with further VES. As well as OBD with another geophysical technique or future deep drilling.

Acknowledgments

To the Facultad de Ciencias Astronómicas y Geofísicas of the Universidad Nacional de La Plata for providing the necessary instrumental and technical support, without which this research would not have been possible.

References

Barends, F. B., Brouwer, F. J., & Schröder, F. H. (eds.). (1995). *Land subsidence* (pp. XI-XIV). Rotterdam, The Netherlands: AA Balkema.

Breiman, L. (2001). Random forests. *Machine Learning*, 45(1), 5-32.

Campo-de-Ferreras, A. M., & Piccolo, M. C. (2002). Hidroquímica del arroyo Pescado Castigado. *Actas III Jornadas Nacionales de Geografía Física*, Santa Fe (p. 97).

Dirección Nacional de Geología y Minería. (1970). *Perfiles de perforaciones* *periodo 1936-1945. Publicación 153, 146.* Argentina: Ministerio de Economía y Trabajo de la Nación.

Domingos, P. (2012). A few useful things to know about machine learning. *Communications of the ACM*, 55(10), 78-87.

García, J. (1969). El agua subterránea en la cuenca del Quequén. *Relatorio de la reunión sobre la geología del agua subterránea de la provincia de Buenos Aires. Comisión de Investigaciones Científicas* (pp. 91-97). La Plata, Argentina.

Giaconi, L. M., Amboni, B. C., & Giaconi, M. N. (2014). Aspectos geológicos y geotécnicos preliminares de la fundación de la presa del Arroyo Blanco, Tandil. *Revista de Geología Aplicada a la Ingeniería y al Ambiente*, (32), 31-52.

González, N. (2005). Los ambientes hidrogeológicos de la Provincia de Buenos Aires. *Relatorio del 16 Congreso Geológico Argentino* (pp. 359-374). La Plata, Argentina.

Harrington, H. J. (1970). Las Sierras Australes de Buenos Aires, República Argentina: Cadena aulacogénica. *Revista de la Asociación Geológica Argentina*, 25(2), 151-181.

Hastie, T., Tibshirani, R., & Friedman, J. (2009). *The elements of statistical learning: Data mining, inference, and prediction*. Springer Science & Business Media. Recuperado de https://hastie.su.domains/Papers/ESLII.pdf

Hernández, M. A., Filí, M., Auge, M., & Ceci, J. H. (1979). Geohidrología de los acuíferos profundos de la Provincia de Buenos Aires. *VI Congreso Geológico Argentino (II)*, Buenos Aires (pp. 479-500).

Johansen, H. K. (1975). An interactive computer/graphic- display-terminal system for interpretation of resistivity soundings. *Geophysical Prospecting*, 23(3), 449-458.

Kruse, E. (1993). El agua subterránea y los procesos fluviales en la región centro oriental de la provincia de Buenos Aires. *Caracterización ambiental de la provincia de Buenos Aires. CIC La Plata*, 2, 15.

Kruse, E., Varela, L., Laurencena, P., & Deluchi, M. (1998). Efectos del agua subterránea en la configuración de los cauces de la llanura interserrana de la provincia de Buenos Aires (Groundwater effects on the stream network in the intermountain plain in the Province of Buenos Aires). In: *Actas del X Congreso Latinoamericano de Geología y VI Congreso Nacional de Geología Económica, Buenos Aires*, 1, 340-344.

Maillet, R. (1947). The fundamental equations of electrical prospecting. *Geophysics*, 12(4), 529-556.

Maiti, S., Gupta, G., Erram, V. C., & Tiwari, R. K. (2011). Inversion of Schlumberger resistivity sounding data from the critically dynamic Koyna region using the Hybrid Monte Carlo-based neural network approach. *Nonlinear Processes in Geophysics*, 18, 179–192, 2011. Recuperado de https://doi.org/10.5194/npg-18-179-2011

Mehta, P., Bukov, M., Wang, C. H., Day, A. G., Richardson, C., Fisher, C. K., & Schwab, D. J. (2019). A high-bias, low-variance introduction to machine learning for physicists. *Physics Reports*, 810, 1-124.

Nigro, J., & Perdomo, S. (2017). Desarrollo de software de inversión de datos 1D para sondeos eléctricos verticales Schlumberger. En: *XXVIII Reunión Científica de la Asociación Argentina de Geofísicos y Geodestas (AAGG 2017) y Tercer Simposio sobre Inversión y Procesamiento de Señales en Exploración Sísmica (IPSES\'17)*. La Plata, del 17 al 21 de abril de 2017.

Nussbaum, M., Spiess, K., Baltensweiler, A., Grob, U., Keller, A., Greiner, L., ... & Papritz, A. J. (2018). Evaluation of digital soil mapping approaches with large sets of environmental covariates. *Soil*, 4(1), 1-

22.

Li, J., Heap, A. D., Potter, A., & Daniell, J. J. (2011). Application of machine learning methods to spatial interpolation of environmental variables. *Environmental Modelling & Software*, 26(12), 1647-1659.

Llambías, E., & Prozzi, C. R. (1975). Ventania. *Geología de la Provincia de Buenos Aires. 6 Congreso Geológico Argentino, Relatorio. Buenos Aires*, 79-101.

Louppe, G. (2014). Understanding random forests: From theory to practice. *arXiv*, preprint arXiv:1407.7502

Orellana, S. E. (1982). *Prospección geoeléctrica en corriente continua. Vol. 1* (2a ed.). Madrid, España: Paraninfo.

Pedregosa, F., Varoquaux, G., Gramfort, A., Michel, V., Thirion, B., Grisel, O.,... & Vanderplas, J. (2011). Scikit-learn: Machine learning in Python. *The Journal of Machine Learning Research*, 12, 2825-2830.

Poland, J. F. (1984). *Guidebook to studies of land subsidence due to ground-water withdrawal*. Studies and reports in hydrology. Recuperado de ttps://unesdoc.unesco.org/ark:/48223/pf0000065167

Prasad, A. M., Iverson, L. R., & Liaw, A. (2006). Newer classification and regression tree techniques: Bagging and random forests for ecological prediction. *Ecosystems*, 9(2), 181-199.

Quiroz-Londoño, O. M., Martínez, D. E., Massone, H. E., Bocanegra, E. M., & Ferrante, A. (2006). Hidrogeología del área Interserrana bonaerense: cuencas de los arroyos El Moro, Tamangueyu y Seco*. 8 Congreso Latinoamericano de Hidrología Subterránea*, Asunción, Paraguay.

Quiroz-Londoño, O. M., Martínez, D., & Massone, H. (2012). Estimación de recarga de acuíferos en ambientes de llanura con base en variaciones de nivel freático. *Tecnología y ciencias del agua*, 3(2), 123-130.

Raj, A. S., Srinivas, Y., Oliver, D. H., & Muthuraj, D. (2014). A novel and generalized approach in the inversion of geoelectrical resistivity data using Artificial Neural Networks (ANN). *Journal of Earth System Science*, 123(2), 395-411.

Ramos, V. A. (1999). Las provincias geológicas del territorio argentino. *Geología Argentina*, 29(3), 41-96.

Sala, J. M. (1975). Recursos hídricos (especial mención de las aguas subterráneas). En: *Relatorio Geología de la Provincia de Buenos Aires. IV Congreso Geológico Argentino.* Buenos Aires, Argentina, (p. 169).

Sala, J. M., & Cavalié, C. C. (1993). *Contribución al mapa geohidrológico de la provincia de Buenos Aires*. Capital Federal, República Argentina: Consejo Federal de Inversiones (CFI).

Sierra, L., Weinzettel, P. A., Dietrich, S., Bea, S., & Cacciabue, L. (septiembre, 2016). Combinación de tomografía eléctrica y perfilaje de pozo para caracterizar variaciones laterales del acuífero pampeano. En: *IX Congreso Argentino de Hidrogeología* y *VII Seminario Hispano-Latinoamericano Sobre Temas Actuales de la Hidrología Subterránea*.

Stefanesco, S., Schlumberger, C., & Schlumberger, M. (1930). Sur la distribution électrique potentielle autour d'une prise de terre ponctuelle dans un terrain à couches horizontales, homogènes et isotropes. *Journal de Physique et le Radium*, 1(4), 132-140.

Sunde, E. D. (1949). *Earth conduction effects in transmission systems*. Dover, UK: Publications Inc.

Terraza, J., & Deguillén, A. (1973). *Nuevos afloramientos paleozoicos de la provincia de Buenos Aires* (trabajo inédito). Bahía Blanca, Argentina: Universidad Nacional del Sur.

Thessen, A. (2016). Adoption of machine learning techniques in ecology and earth science. *One Ecosystem*, 1, e8621.

Varni, M., Weinzettel, P., & Usunoff, E. (2010). Caracterización hidrodinámica e hidroquímica de la cuenca del Arroyo Claromecó, provincia de Buenos Aires. Buenos Aires, Argentina: Consejo Hídrico Federal.

Weinzettel, P., Varni, M., & Usunoff, E. (2005). Caracterización hidrogeológica del área urbana y periurbana de la ciudad de Tres Arroyos, provincia de Buenos Aires. En: *Actas. IV Congreso Argentino de Hidrogeología. Río Cuarto, Córdoba* (vol. 25, pp. 171-180).

Weinzettel, P. A., & Varni, M. (2007). Aporte al conocimiento del subsuelo de la cuenca del arroyo Claromecó, provincia de Buenos Aires. *Taller de Geofísica Aplicada a la Hidrogeología*, 13-23.

Zohdy, A. A. (1989). A new method for the automatic interpretation of Schlumberger and Wenner sounding curves. *Geophysics*, 54(2), 245-253.